International Journal of Refrigeration 105 (2019) 158–168

Contents lists available at ScienceDirect

International Journal of Refrigeration

journal homepage: www.elsevier.com/locate/ijrefrig

Thermal conductivity of AQSOA FAM-Z02 packed bed adsorbers in open and closed adsorption thermal energy storage systems

Mina Rouhani, Wendell Huttema, Majid Bahrami*

Laboratory for Alternative Energy Conversion (LAEC), School of Mechatronic Systems Engineering, Simon Fraser University, BC V3T0A3, Canada

ARTICLE INFO

Article history:
Available online 18 May 2018

Keywords:
Effective thermal conductivity
Thermal contact resistance
AQSOA FAM-Z02
Packed bed adsorber
Closed and open adsorption systems
Adsorption thermal energy storage

ABSTRACT

In this study, the effective thermal conductivity (ETC) of uniformly-sized packed bed adsorber is modeled as a function of water uptake, number of adsorbent layers, particle size, bed porosity, temperature, contact pressure, and interstitial gas pressure. The model is validated against experimental data for 2 mm AQSOA FAM-Z02, measured by heat flow meter method (ASTM standard C518), and the maximum relative differences between the predicted values and the experimental data are 2% for ETC and 8% for total thermal conductivity. For 0.32 kg kg_{ads}^{-1} water uptake, at 30 °C, ETC of an open-system 2 mm FAM-Z02 SC-arranged packed bed adsorber is 2.2 times higher than the ETC of a closed-system (0.1031 W m^{-1} K^{-1} compared to 0.0474 W m^{-1} K^{-1}). ETC charts are presented based on the equilibrium water uptake isotherms for 0.5 and 2 mm FAM-Z02 packed beds, which provides a detailed and clear picture of ETC of packed bed adsorbers for both open and closed thermal energy storage applications. For each packed bed storage volume, an optimum particle size can be predicted by the presented model, which ensures the highest packed bed total thermal conductivity.

Conductivité thermique des adsorbeurs à garnissage AQSOA FAM-Z02 dans les systèmes ouverts et fermés de stockage d'énergie thermique par adsorption

Mots-clés: Conductivité thermique efficace; Résistance thermique de contact; AQSOA FAM-Z02; Adsorbeur à garnissage; Systèmes à adsorption fermés et ouverts; Stockage d'énergie thermique par adsorption

1. Introduction

To reduce primary energy demand and greenhouse gas emissions, adsorption systems, including adsorptive heat transformers (Frazzica et al., 2014; Freni et al., 2015) and adsorption thermal energy storage (ATES) systems (Li et al., 2014; Schreiber et al., 2015), have received increased attention in recent years. However, the low thermal conductivity of adsorbent materials, 0.1–0.8 W m^{-1} K^{-1} (N' Tsoukpoe et al., 2014), and high thermal contact resistance (TCR) between the adsorbent materials and adsorber bed metal surfaces suppress the overall performance of adsorption systems, through slow desorption and adsorption processes. To investigate and improve the heat transfer performance of adsorption systems, effective thermal conductivity (ETC) of the adsorber beds as well as the TCR, should be measured and modeled properly. Since it is costly and difficult to run thermal conductivity measurements in large-scale for varying particle size, number of layers, filling gas pressure, relative humidity (RH), contact pressure, water uptake and temperature, a reliable comprehensive model for thermal conductivity is vital to accurately analyze, predict, and improve the thermal performance of adsorption systems.

Exploiting heat sources with intermittent nature (e.g. renewables and waste heat) and matching it with the demand side make thermal energy storage (TES) an effective method for reducing the fossil fuel dependency and carbon emissions (Cabeza, 2014). High energy storage density, low heat loss and using non-toxic and non-polluting refrigerants make adsorption TES (ATES) more appealing and effective for heat/cold storage, compared to other thermal storage methods (Cabeza, 2014; Yu et al., 2013). Packed bed

* Corresponding author.
E-mail addresses: mrouhani@sfu.ca (M. Rouhani), wah@sfu.ca (W. Huttema), mbahrami@sfu.ca (M. Bahrami).

https://doi.org/10.1016/j.ijrefrig.2018.05.012
0140-7007/

Nomenclature

A	heat transfer surface area of the packed bed, m^2
A_{cell}	heat transfer surface area of the unit cell, m^2
ATES	adsorption thermal energy storage
a_{macro}	radius of macro-contact, mm
a_H	radius of Hertzian contact, mm
α_T	thermal accommodation coefficient
b_{macro}	chord of macro-contact, mm
β	volume fraction
d_p	adsorbent particle diameter, mm
d_v	Vickers indentation diagonal, μm
ε	adsorbent particle porosity
E_p	Young's modulus of adsorbent particle, GPa
ETC	effective thermal conductivity
F	contact force, N
FCC	face center cubic arrangement
k	thermal conductivity, W m^{-1} K^{-1}
$k_{eff,\ bed}$	packed bed effective (medium) thermal conductivity (effects of TCR is not included.), W m^{-1} K^{-1}
$k_{eff,\ FCC}$	FCC-arranged packed bed effective thermal conductivity (effects of TCR is not included.), W m^{-1} K^{-1}
$k_{eff,\ SC}$	SC-arranged packed bed effective thermal conductivity (effects of TCR is not included.), W m^{-1} K^{-1}
k_g	adsorbate gas thermal conductivity, W m^{-1} K^{-1}
k_{ha}	humid air thermal conductivity, W m^{-1} K^{-1}
k_p	adsorbent particle thermal conductivity, W m^{-1} K^{-1}
k_{tot}	packed bed total thermal conductivity (effects of TCR is included.), W m^{-1} K^{-1}
k_v	water vapour thermal conductivity, W m^{-1} K^{-1}
L_{b-cell}	boundary unit cell length, mm
L_{bed}	packed bed length (thickness), mm
L_{cell}	unit cell length, mm
m	number of adsorbent particles in each adsorbent layer
m_{ads}	adsorbent mass, kg
n	number of layers of adsorbent particles
r	adsorbent particle radius, mm
ρ_p	radius of adsorbent sphere, m^{-1}
ρ_s	density of solid adsorbent, kg m^{-3}
ρ_w	density of adsorbate water, kg m^{-3}
ν_p	Poisson's ratio of adsorbent particle
ω	water uptake, kg kg_{ads}^{-1}
ω_{eq}	equilibrium water uptake, kg kg_{ads}^{-1}
P	gas pressure, Pa
P_0	maximum contact pressure, Pa
P_0'	relative maximum contact pressure, Pa
$P_{0,\ H}$	Hertzian pressure, Pa
P_{ref}	reference gas pressure, Pa
$P_{contact}$	contact pressure at the contact of adsorbent particle and the metal surface, Pa
P_{sat}	saturation pressure, Pa
$\dot{Q}$	heat flow, W
$\dot{Q}_{C,macro}$	macro-contact heat flow, W
$\dot{Q}_{c,micro}$	micro-contact heat flow, W
$\dot{Q}_{g,micro}$	micro-gap heat flow, W
$\dot{Q}_{G,macro}$	macro-gap heat flow, W
R	thermal resistance, K- W^{-1}
R_{bed}	packed bed medium thermal resistance (effect of TCR is not included), K W^{-1}
R_{cell}	unit cell thermal resistance, K W^{-1}
$R_{C,\ macro}$	macro-contact thermal resistance, K W^{-1}
$R_{c,\ micro}$	micro-contact thermal resistance, K W^{-1}
$R_{g,\ micro}$	micro-gap thermal resistance, K W^{-1}
$R_{G,\ macro}$	macro-gap thermal resistance, K W^{-1}
R_p	adsorbent particle thermal resistance, K W^{-1}
R_{tot}	packed bed total thermal resistance (effect of TCR is included), K W^{-1}
RH	relative humidity, %
SC	simple cubic arrangement
ψ_{bed}	packed bed solid fraction
ψ_{FCC}	FCC-arranged packed bed solid fraction
ψ_{SC}	SC-arranged packed bed solid fraction
T	temperature, K
TCR	thermal contact resistance, K W^{-1}

Subscripts

a	air
ads	adsorbent
bed	packed bed
$cell$	cell
$closed$	closed sorption storage system
$contact$	at the contact of adsorbent particles and the heat exchanger metal surface
eff	effective
FCC	FCC arrangement
g	adsorbate gas
ha	humid air
$open$	open sorption storage system
p	adsorbent particle
s	solid particle (adsorbent skeleton)
SC	SC arrangement
tot	total
v	water vapour
w	water
wet	wet adsorbent particle

adsorbers are widely used in adsorption systems (Aristov et al., 2012; El-Sharkawy et al., 2013; Pistocchini et al., 2016; Ramzy K et al., 2011; Hauer and Fischer, 2011; Palomba et al., 2017), since they provide higher cooling/heating energy per volume and benefit from lower cost and complexity, compared to the coated or consolidated adsorber beds (Freni et al., 2015; Freni et al., 2015). A monolayer configuration of adsorption beds ensures less heat transfer resistance and higher water uptake rate, although multi-layers are more desirable for storage applications, due to the higher metal-to-adsorbent mass ratio (active mass) and lower coefficient of performance of the monolayer configuration (N' Tsoukpoe et al., 2014). These two competing trends indicate a need for further investigation to establish optimum configurations (number of layers of adsorbents and packed bed arrangements).

Importance of TCR in adsorber beds has been raised in the literature (Rezk et al., 2013; Li et al., 2015; Sharafian et al., 2014), but only adsorbent thermal conductivity or adsorber bed ETC are taken into account in most adsorption models. In the lumped-parameter thermodynamic models, heat transfer in the adsorber bed heat exchanger is modeled through an overall heat transfer coefficient of the heat exchanger, and adsorption rate constant represents the heat and mass transfer performance of an adsorption system (Alsaman et al., 2017). Mohammed et al. (2017) developed a three-dimensional local thermal non-equilibrium model, where ETC was assumed constant. In other theoretical models (Riffel et al., 2010; Rezk and Al-Dadah, 2012), measured TCR values from the experiments were fed into the model. Rezk and Al-Dadah (2012) presented a lumped analytical model for predicting ETC of a silica gel packed bed, where they used a correlation for the TCR, which was fitted to the measured TCR in ref. Zhu and Wang (2002).

Analytical and numerical solutions to the Laplace's equation are the first type of ETC models (VDI Heat Atlas 2010). Maxwell analytical solution, which is based on the assumption of no thermal influence between individual particles, falls in this category (VDI Heat Atlas 2010). On the other hand, numerical models of packed bed thermal conductivity, which do not need such limiting assumptions, suffer from high computational cost and time.

Another type of ETC models is introducing thermal resistance network for the packed bed adsorber (VDI Heat Atlas 2010). Griesinger et al. (1999) experimentally and theoretically studied the ETC of zeolite powder at atmospheric pressure by introducing three main parallel heat transfer paths (pure solid, pure fluid, and mixed solid-fluid paths) and defining tuning parameters through fitting the theoretical curve to the measured values (Griesinger et al., 1999). Similarly, Dawoud et al. (2011) developed a model to calculate the ETC of wetted zeolite 4A, assuming an isotropic distribution of adsorbed water inside the zeolite crystal. A tortuosity factor was defined for conductive heat transfer and their model took into account the Knudsen conductivity of the vapor phase through the curve fitting to their experimental data (Dawoud et al., 2011). Nevertheless, ETC models of small amount of adsorbent samples, i.e. an adsorbent particle or powder, may not be an accurate representative of a large-scale packed bed adsorber, since they do not take into account all the thermal resistances inside the packed bed, including the thermal resistance between the adsorbent particles as well as the TCR.

Thermal conductivity modeling of a unit cell (as a representative of the repeating units in a packed bed), by using thermal resistance network or basic models such as Maxwell, is another type of ETC models for packed beds (VDI Heat Atlas 2010). Luikov et al. (1968) defined a thermal resistance circuit for a unit cell, which contained a solid skeleton and surrounding gas, although the boundary unit cell and water uptake were not considered in their study. In addition to their model, Sarwar and Majumdar (1995) took into account the effects of the adsorbent water content on a packed bed ETC, although interstitial gas pressure and the contact pressure were not considered as variables in their model.

Bahrami et al. (2006) developed an analytical unit-cell model for ETC of uniformly-sized packed beds with high-conductive spheres. Rouhani and Bahrami (2018) used their analytical model as a platform for dry packed beds, and extended it to consider the effects of water uptake in the packed bed adsorbers. In this work, the developed model in ref. Rouhani and Bahrami (2018), inclusive of considering the effects of air relative humidity on the air thermal conductivity of the open systems, is used to investigate and compare open and closed-system packed bed ATES systems. The present model can predict the ETC and TCR of packed bed adsorbers as a function of:(i) numbers of adsorbent layers, (ii) adsorbent properties, (iii) particle size, (iv) water uptake, (v) temperature, (vi) contact pressure, (vii) particles surface roughness, (viii) particle arrangement and (ix) interstitial gas pressure. This model provides a practical tool to analysis, optimize and compare thermal performances of open and closed packed bed adsorbers, under various operating conditions.

2. Theoretical model

A unit cell approach is adopted, considering a unit-cell as the representative of a uniformly-arranged simple cubic (SC) packed bed, as shown in Fig. 1a. In contrast to the model presented by Bahrami et al. (2006), which was for high conductive particles, adsorbent particle thermal resistance is considered in the present model, due to the high thermal resistance of adsorbent materials. Thermal conductivities of wet adsorbent particles are modeled by an effective-medium approximation of multi-component systems, Bruggeman's method.

Natural convection in the small voids between the particles in the packed beds can be neglected (Tsotsas and Martin, 1987). Moreover, in the model and the experimental data (Rouhani et al., 2018), the heat flow is downward to eliminate the natural convection (Incropera et al., 2007; Czichos et al., 2011). In the packed beds for low-temperature applications radiation is also negligible (Yovanovich, 2003). Therefore, heat transfer occurs via conduction through the solid adsorbent and conduction through the interstitial gas, as shown in Fig. 1b. These conductive heat transfer mechanisms take place in multi-scales: (i) macroscale, including macro-contact ($\dot{Q}_{C,macro}$) and macro-gap ($\dot{Q}_{G,\ macro}$) paths; and (ii) microscale, including micro-contact ($\dot{Q}_{c,micro}$) and micro-gap ($\dot{Q}_{g,\ micro}$) paths.

It is assumed that the steady-state condition is reached for both heat and mass transfer; therefore, the water uptake of the adsorbent particles is corresponded to the equilibrium water uptake at the steady-state temperature and pressure ratio ($P/P_{sat@T_{ads}}$).

A wet adsorbent particle is an inhomogeneous medium of three components: (i) solid particle (adsorbent skeleton), (ii) adsorbed water on the surface of adsorbent pores, and (iii) interstitial gas, which is the air in the open adsorption systems and water vapor in the closed adsorption systems. Among various models of effective-medium approximation, Bruggeman's method for multi-component medium is selected, since it is readily applicable to arbitrary volume fractions (Stroud, 1998). Therefore, the thermal conductivity of a wet adsorbent particle, $k_{p,\ wet}$, can be calculated as follows,

$$\sum_{i=1}^{3} \beta_i \frac{k_i - k_{p,wet}}{k_i + 2k_{p,wet}} = 0, \quad \text{where} \ \sum_{i=1}^{3} \beta_i = 1 \tag{1}$$

where β_i is the volume fraction of each component. Volume fraction of solid particle, water and gas are obtained from Eq. (2).

$$\begin{aligned} \beta_s &= 1 - \varepsilon \\ \beta_w &= \omega \frac{\rho_s}{\rho_w}(1 - \varepsilon) \\ \beta_g &= \varepsilon - \omega \frac{\rho_s}{\rho_w}(1 - \varepsilon) \end{aligned} \tag{2}$$

where ε is the porosity of the adsorbent particle and ρ_s is the pore-less density of the adsorbent material.

ETC of the packed bed adsorber is calculated based on the unit cell approach and it is assumed that the heat conduction in the unit cell is one dimensional, which leads to isothermal top and bottom surfaces, while the lateral walls are adiabatic due to symmetry (see Fig. 1a) (Bahrami et al., 2006). As shown in Fig. 1b, the thermal resistance of the unit cell consists of: (1) bulk thermal resistance of particles, R_p, (2) macro-contact constriction/spreading resistance, $R_{C,\ macro}$, (3) micro-contact constriction/spreading resistance, $R_{c,\ micro}$, (4) resistance of the interstitial gas in the micro-gap, $R_{g,\ micro}$, and (5) resistance of interstitial gas in the macro-gap, $R_{G,\ macro}$. The equations used in this study are presented in Appendix A, and more details are found in ref. Bahrami et al. (2006).

Thermal and physical properties of the adsorbent material, including thermal accommodation, $\alpha_{T,\ p}$, and Young's modulus, E_p (see Appendix A) are required for the ETC calculations. In this model, a clean surface is assumed for the adsorbent particle, therefore, the correlation for thermal accommodation of clean surfaces, developed by Song and Yovanovich (1987), is applied (see Eq. A 24 in Appendix A). A thermomechanical analyzer (TMA Q400EM from TA Instruments) with precision of $\pm 0.1\%$ was used to measure the Young's modulus of 2-mm FAM-Z02 adsorbent particle (Rouhani and Bahrami, 2018). The value of 0.5736 GPa^{-1} was obtained for $(1 - \nu_p^2)/E_p$ (see Eq. A 18 in Appendix A), where ν_p is particles Poisson's ratio and E_p is particles Young's modulus (Rouhani and Bahrami, 2018). Using the proposed unit cell thermal resistance

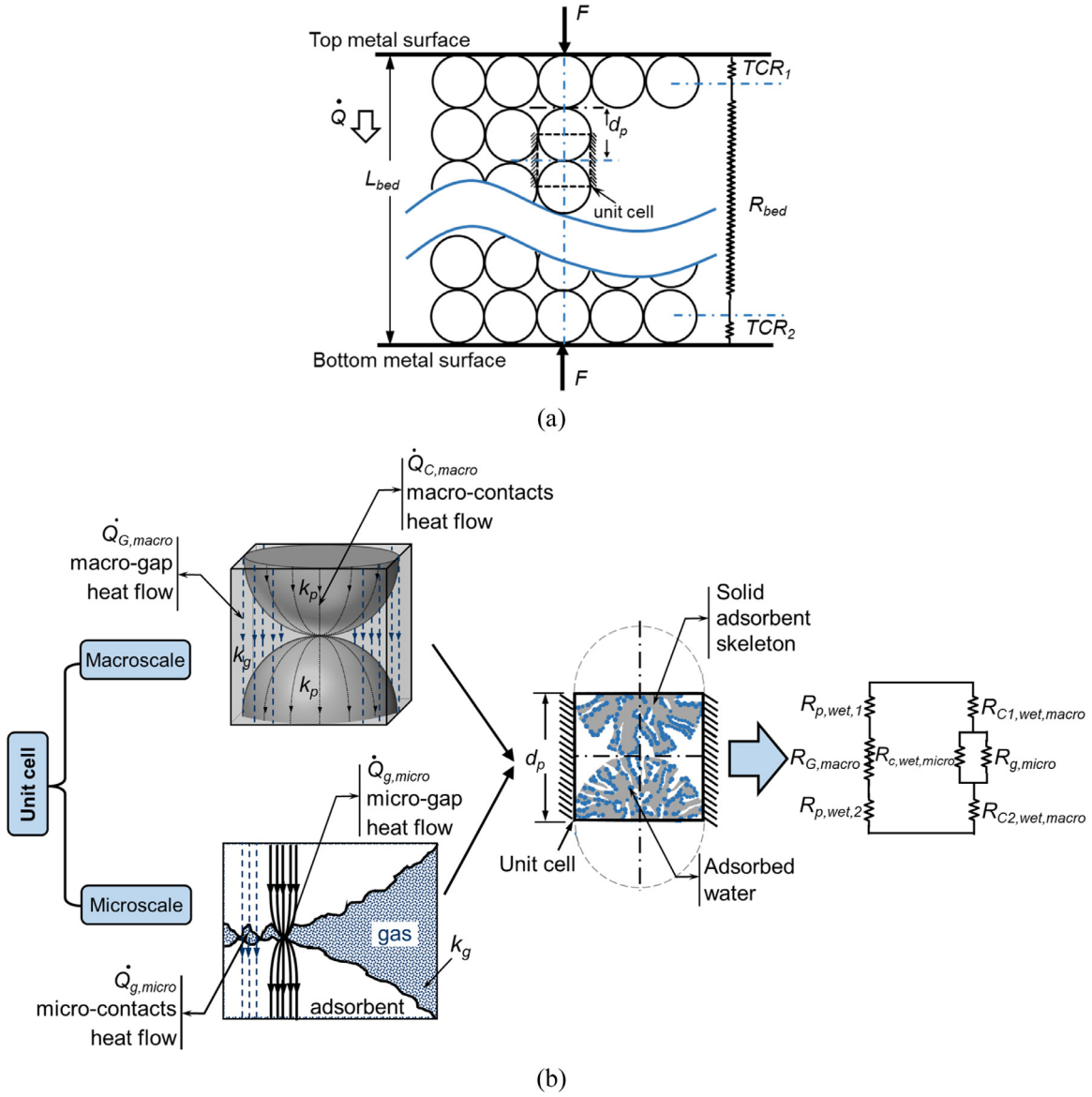

Fig. 1. (a) Packed bed adsorber of adsorbents with diameter of d_p, for simple cubic (SC) arrangement (Bahrami et al., 2006), and (b) heat conduction in the packed bed, shown in macro-scale and micro-scale, and a unit cell of a wet SC-arranged adsorber bed with the equivalent electrical circuit.

network, shown in Fig. 1b, the total thermal resistance of the unit cell is as follows,

$$R_{cell} = \left[\frac{1}{\left(1/R_{c,micro} + 1/R_{g,micro}\right)^{-1} + R_{C,macro}} + \frac{1}{R_p + R_{G,macro}} \right]^{-1} \tag{3}$$

The unit cell ETC can be calculated from $k_{eff,cell} = L_{cell}/(R_{cell}A_{cell})$, which is also the ETC of the packed bed ($k_{eff,\ bed}$), considering a homogenous medium. Thermal resistances of the unit cells along the bed's length (i.e. in the heat transfer direction) are in series, while they are parallel to each other in the direction perpendicular to the heat transfer path. Thus, the thermal resistance of adsorber medium is $R_{bed} = [L_{bed}/(k_{eff,bed}\ A_{cell})]/m$, where L_{bed} is the bed length in the heat transfer direction and m is the number of unit cells in each layer of the adsorber bed.

The TCR in the unit cells adjacent to the two metal surfaces of heat exchanger medium, are also in series with the medium resistance (R_{bed}). Thus, the total bed resistance is $R_{tot} = R_{bed} + TCR$. To this end, the total thermal conductivity of a packed bed can be found from:

$$k_{tot} = \frac{L_{bed}}{A\ (R_{bed} + TCR)} \tag{4}$$

where, $A = A_{cell} \times m$ is the total area of the metal surface. Similarly, all the thermal resistances of the adsorbent particle side and the gas side are calculated for the face center cubic (FCC) arrangement, using related equations in ref. Bahrami et al. (2006) and the parameters in Table 1, for FCC arrangement.

The ETC of a randomly packed bed ($\psi_{bed} \approx 0.6$ (Kaviany, 1995)) falls between that of the two uniformly-sized, uniformly-packed arrangements: SC ($\psi_{bed} = 0.524$), as the lower bound, and FCC ($\psi_{bed} = 0.740$), as the upper bound (Tien and Vafai, 1978; Karayacoubian et al., 2005). Therefore, by assuming a linear relationship using the ETC values of SC and FCC arrangements, ETC of the randomly packed bed can be estimated based on its solid fraction, as follows,

$$\frac{\psi_{bed} - \psi_{SC}}{\psi_{FCC} - \psi_{SC}} = \frac{k_{eff,bed} - k_{eff,SC}}{k_{eff,FCC} - k_{eff,SC}} \tag{5}$$

Table 1
Specifications of SC and FCC arrangements of a packed bed.

Packing arrangement	Solid fraction, ψ_{bed}	Bed length, L_{bed}	Cell area, A_{cell}	Cell length, L_{cell}	Boundary cell length, L_{b-cell}
SC	0.524	$n \times d_p$	d_p^2	d_p	$d_p/2$
FCC	0.740	$((n-1)\sqrt{2}/2+1) \times d_p$	$d_p^2/2$	$\sqrt{2}d_p/2$	$d_p/2$

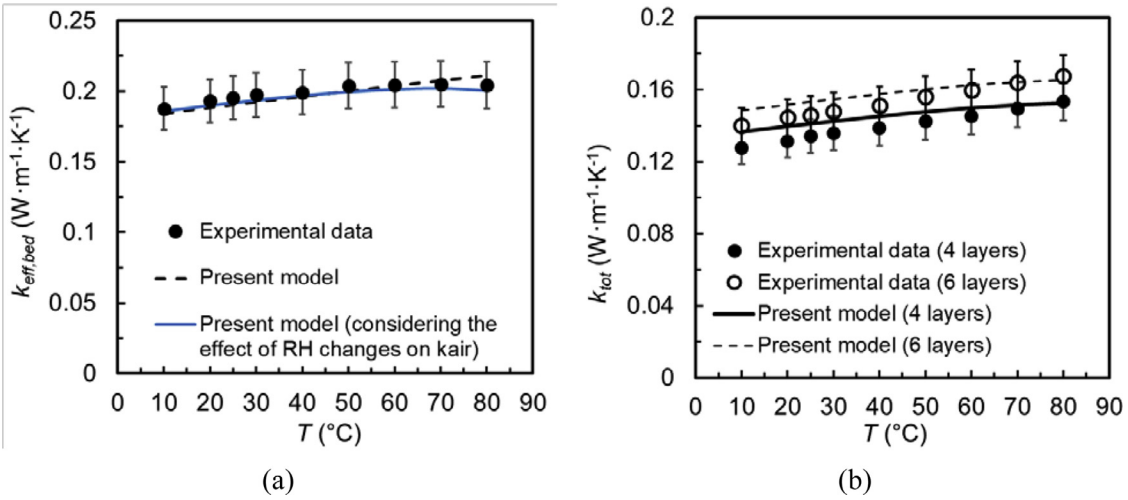

Fig. 2. (a) Effective thermal conductivity and (b) total thermal conductivity of 4- and 6-layer packed beds versus temperature for 2-mm FAM-Z02 randomly packed beds with the water uptake of 0.30 ± 0.02 kg kg_{ads}^{-1}, at atmospheric condition and under contact pressure of 0.7 kPa. In the present model, ψ_{bed} is 0.67.

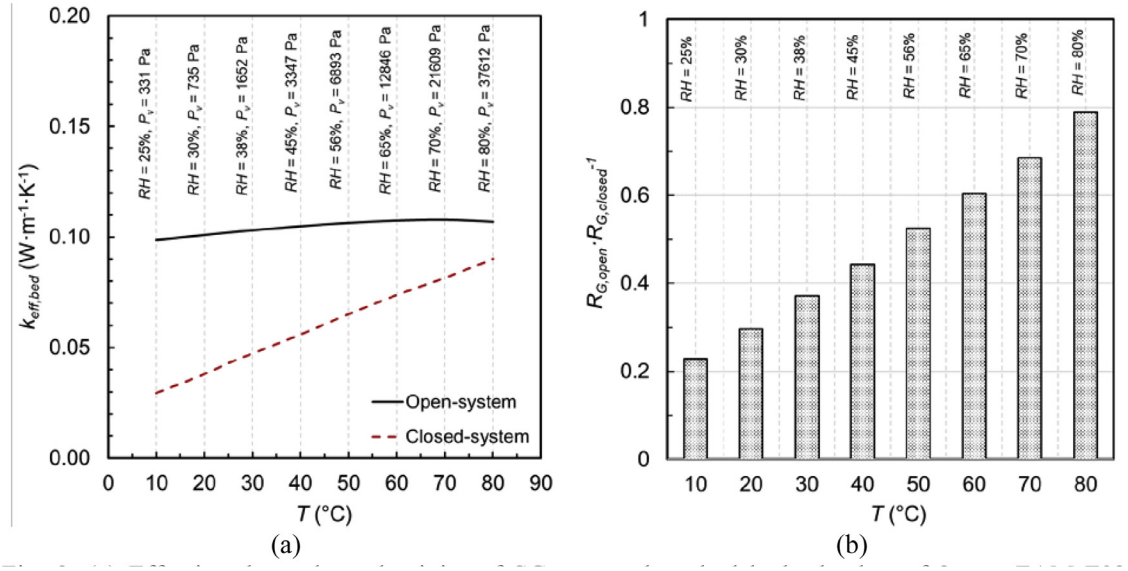

Fig. 3. (a) Effective thermal conductivity of SG-arranged packed bed adsorber of 2 mm FAM-Z02 versus temperature, for open and closed-systems, at equilibrium water uptake of 0.32 kg kg_{ads}^{-1} and (b) the ratio of the macro-gap resistances of open-system to that of the closed-system.

where, ψ_{SC}, ψ_{FCC} and ψ_{bed} are the solid fractions of the SC, FCC and any randomly packed bed arrangements, respectively. Solid fraction of a randomly packed bed adsorber can be assumed about 0.62 (porosity of 0.38 (Do, 1998)) or can be chosen such that $k_{eff,\,bed}$ approaches the experimental data collected for thermal conductivity of that randomly packed bed (Rouhani and Bahrami, 2018; Rouhani et al., 2018).

3. Results and discussion

3.1. Model validation

The present ETC model is coded into MATLAB in four sections: (i) water uptake calculation from the equilibrium isotherms, reported by Goldsworthy (2014), (ii) adsorbent particle thermal resistance model, (iii) packed bed cell resistance, and (iv) packed bed boundary cell resistance models. The ETC model is then compared with the measured values of refs. Rouhani et al. (2018); (2016), where a heat flow meter (HFM) apparatus was used to measure the total thermal conductivity of large-scale 2-mm FAM-Z02 randomly packed beds, at adsorbent temperatures from 10 to

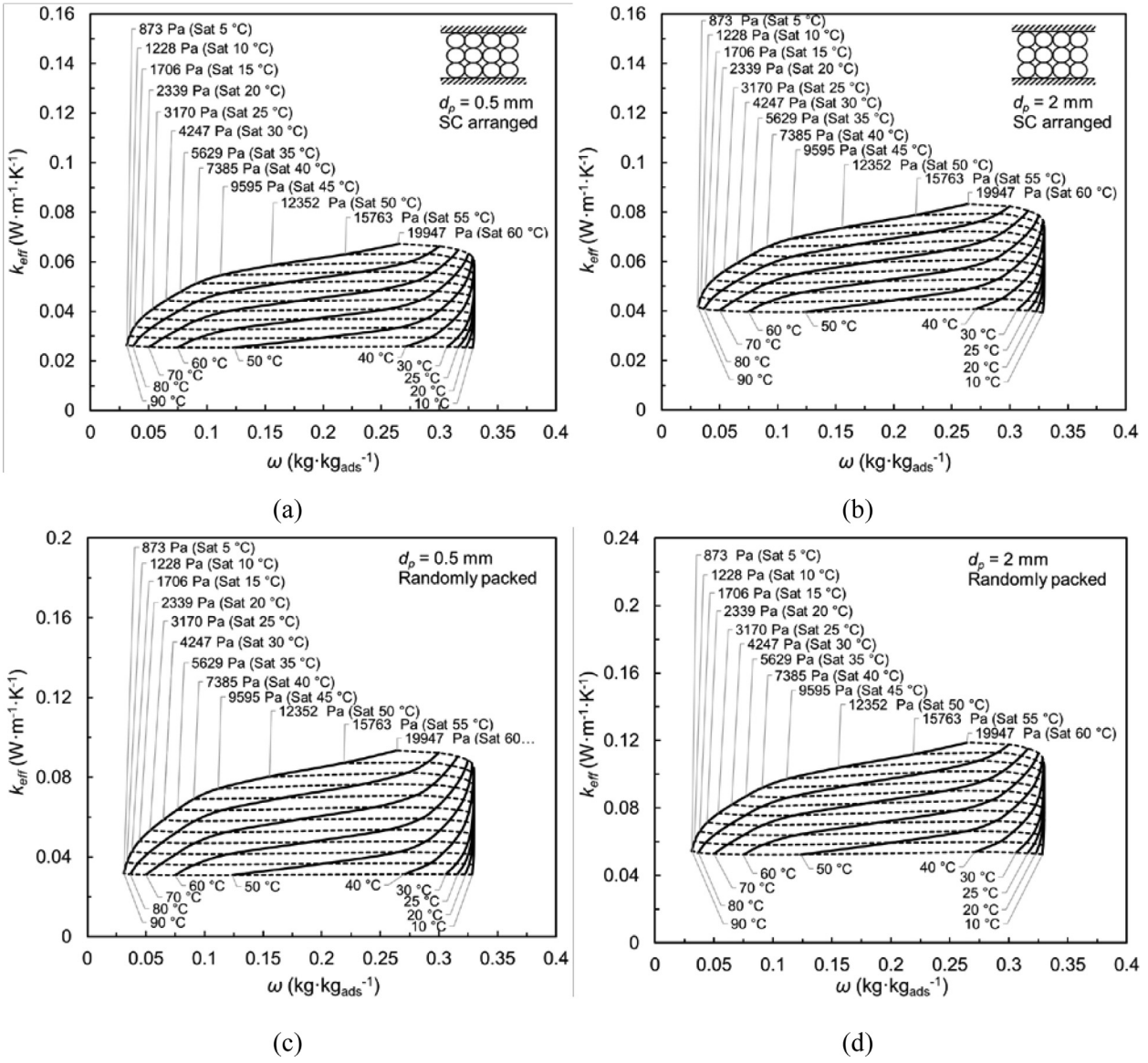

Fig. 4. Effective thermal conductivity of closed-system FAM-Z02 packed bed adsorber versus water uptake, including the isotherm and isobar lines for (a) SC-arranged bed with 0.5 mm adsorbent particles, (b) SC-arranged bed with 2 mm adsorbent particles, (c) randomly packed bed with 0.5 mm adsorbent particles, and (d) randomly packed bed with 2 mm adsorbent particles.

80 °C. The packed beds were sandwiched between two aluminum sheets and placed in the test chamber between two plates with heat flow transducers in their center (Rouhani et al., 2018). An external load was applied by the HFM on the packed bed, to control the contact pressure and ensure a uniform contact between the upper (hot)/lower (cold) plates and the packed adsorbent particles (Rouhani et al., 2018; 2016). The comparison between the experimental values and the present model for ETC is shown in Fig. 2a, for a 2-mm FAM-Z02 randomly packed bed. The black dashed line represents the results of the present model, where the air thermal conductivity is approximated as the thermal conductivity of dry air, and the blue solid line shows the results from the model, where the effect of RH changes on the air thermal conductivity is also considered; thermal conductivity of humid air, as a function of RH, is calculated from the equations presented in Table B1 of Appendix B, using the mole-fraction-weighted mixing rule. As shown in Fig. 2a, the present model can predict $k_{eff,\ bed}$ accurately and the agreement between the experimental data (Rouhani et al., 2018) and the results from the present model has been improved by considering the effect of the RH changes, due to the temperature changes, on the air thermal conductivity; in the experimental study (Rouhani et al., 2018), RH was 25% (at 10 °C) and 80% (at 80 °C) for constant water uptake of 0.30 ± 0.02 kg kg$_{ads}^{-1}$. For temperatures above 60 °C and RH values above 50%, an increase in RH decreases the thermal conductivity of humid air (see the equation for k_{ha} in Table B1 of Appendix B). This decrease in the air thermal conductivity marginally decreases the ETC compared to the case where the effects of the changes in RH are not considered. The maximum relative difference between the results from the model without consideration of RH changes and the experimental data is 3% at 80 °C, while the maximum relative difference is 2% with consideration of RH changes at 80 °C. ETC of the packed bed adsorber varies between 0.188 and 0.204 W m^{-1} K^{-1}. Total thermal conductivities of the packed beds of 4 and 6 layers of 2 mm FAM-Z02 are shown in Fig. 2b. The theoretical model can properly predict the total thermal conductivity, which includes the TCR as well. The maximum difference between the experimental data and the results from the theoretical model is 8% and lies within the uncertainty of the measurements.

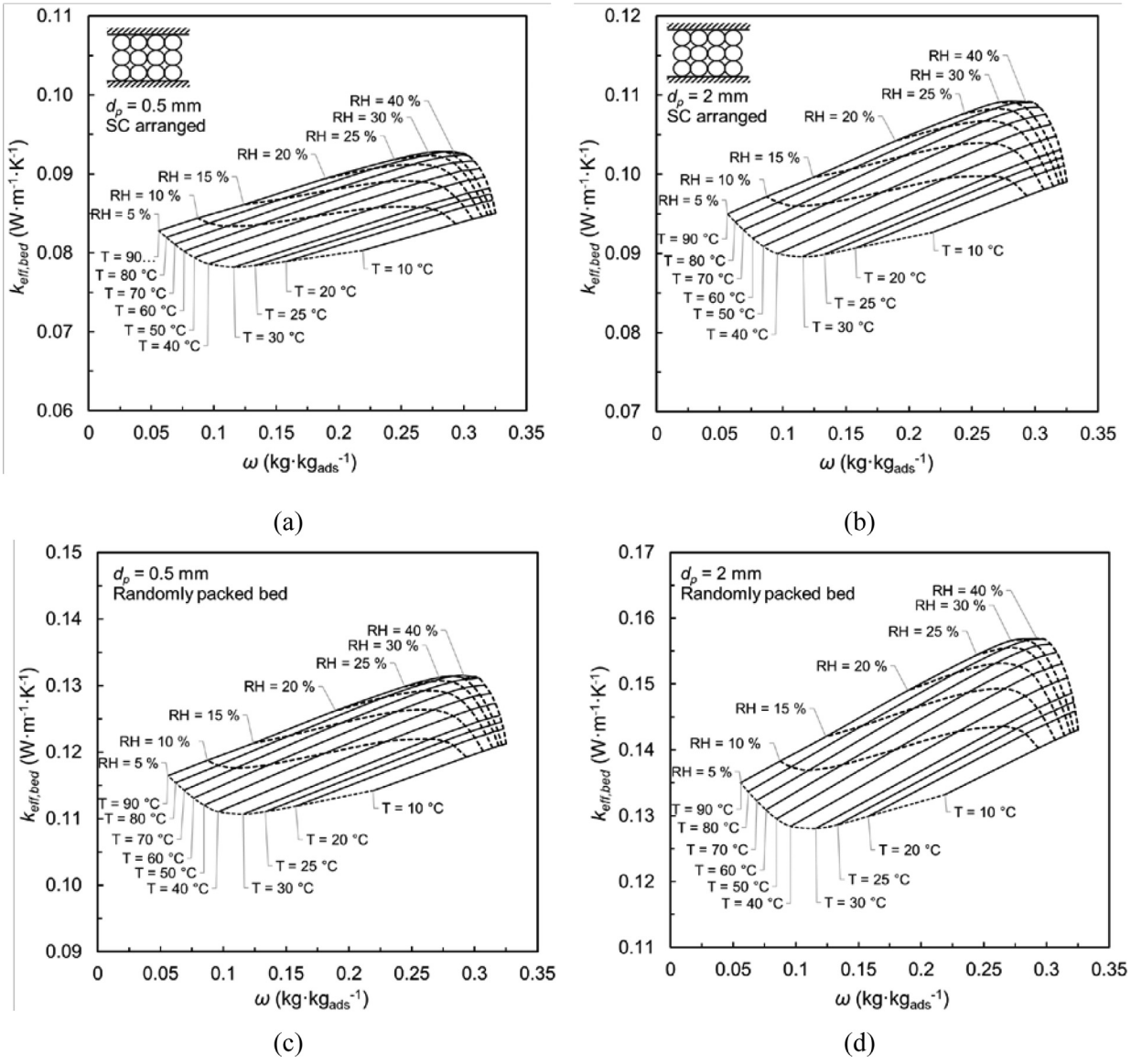

Fig. 5. Effective thermal conductivity of open-system FAM-Z02 packed bed adsorbers versus water uptake, including the isotherm and isobar lines for (a) SC-arranged bed with 0.5 mm adsorbent particles, (b) SC-arranged bed with 2 mm adsorbent particles, (c) randomly packed bed with 0.5 mm adsorbent particles, and (d) randomly packed bed with 2 mm adsorbent particles.

3.2. Effective thermal conductivity: open-system versus closed-system packed bed adsorbers

ETCs of open and closed-system packed bed adsorbers of 2 mm FAM-Z02 at equilibrium water uptake of 0.32 kg kg$_{ads}^{-1}$, are shown in Fig. 3a. According to the water uptake isotherms (Goldsworthy, 2014), the RH changes from 25% to 80% for temperatures of 10 to 80 °C. As shown in Fig. 3a, ETC of open-system is 3.3 times as high as ETC of the closed-system (0.099 compared to 0.030 W m^{-1} K^{-1}) at 10 °C, and 1.2 times as high as that of the closed system (0.107 compared to 0.090 W m^{-1} K^{-1}) at 80 °C. Although the water uptake is kept the same for both open and closed systems, the gas pressure around the adsorbents in the closed-system is much lower and varies from 331 Pa (at 10 °C) to 37,612 Pa (at 80 °C). The ratio of macro-gap resistances of the open-system to that of the closed-system, in Fig. 3b, shows that the low gas pressure in the closed-system leads to relatively high macro-gap resistances, especially at lower temperatures. The $R_{G,\ open}/R_{G,\ closed}$ is 0.23 at 10 °C (331 Pa) and 0.79 at 80 °C (37,612 Pa).

3.3. Effective thermal conductivity chart for closed-system packed bed adsorbers

The dependencies of the ETC on the water uptake, vapour pressure, and mean temperature are shown in Fig. 4 for SC-arranged and randomly packed beds ($\psi_{bed} = 0.6$) of 0.5 and 2 mm FAM-Z02. To consider the real effects of water uptake, pressure and temperature on the ETC in closed adsorption systems, the water uptake is calculated at each temperature and pressure ratio from the equilibrium uptake isotherms of FAM-Z02, presented by Goldsworthy (2014). Afterwards, using the present model, the ETC is obtained based on the pressure, temperature and water uptake, forming the isobars and isotherms in Fig. 4. ETCs are reported for the temperatures of 10 to 90 °C, pressures of 873 (saturation pressure at 5 °C) and 19,947 Pa (saturation pressure at 60 °C), and water uptakes of 0.03 to 0.33 kg kg$_{ads}^{-1}$. As shown in Fig. 4, at a fixed gas pressure, ETC does not significantly change with the changes in temperature and water uptake; at a constant pressure, an increase in temperature leads to a decrease in the equilibrium

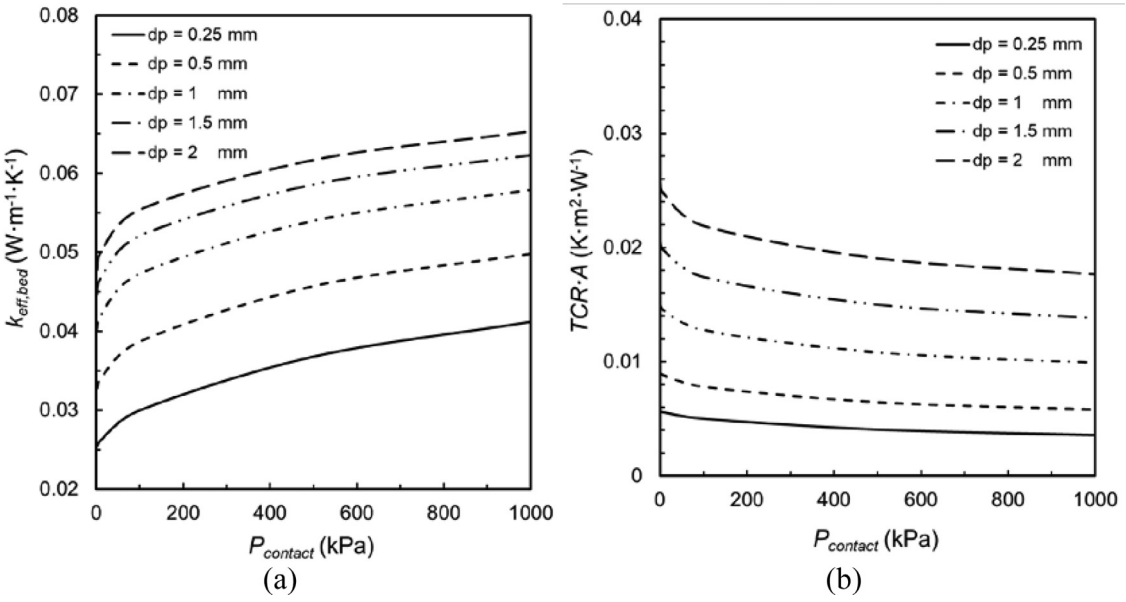

Fig. 6. (a) ETC and (b) $TCR \cdot A$ of a closed-system SC-arranged packed bed adsorber versus contact pressure for various particle diameters, at 30 °C and 1706 Pa ($\omega_{eq} = 0.32$ kg kg_{ads}^{-1}). L_{bed} is fixed at 12 mm.

water uptake. Temperature rise increases the ETC, while water uptake drop decreases the ETC. The tradeoff between these two effects results in an almost constant ETC. However, at a fixed temperature, equilibrium water uptake increases with an increase in gas pressure and both increases positively affect the ETC. At 90 °C, by increasing the gas pressure from 872 Pa ($\omega_{eq} = 0.03$ kg kg_{ads}^{-1}) to 19,947 Pa ($\omega_{eq} = 0.26$ kg kg_{ads}^{-1}), ETC increases from 0.027 to 0.068 W m^{-1} K^{-1} for 0.5 mm, and from 0.044 to 0.084 W m^{-1} K^{-1} for 2 mm SC-arranged packed beds. Considering the equilibrium uptake isotherms, it can be concluded that ETC is a stronger function of vapor pressure than temperature in closed systems, for the studied temperature and pressure ranges. Higher thermal conductivities have been predicted for randomly packed beds compared to the SC-arranged beds, due to the lower bed porosity of randomly packed beds, which makes thermal conductivity of adsorbent particle to take higher part in the ETC; thermal conductivity of the adsorbent, i.e. 0.117 W m^{-1} K^{-1} (at 30 °C) and 0.128 W m^{-1} K^{-1} (at 90 °C) (Kakiuchi et al., 2004), is higher than that of the water vapor, i.e. 0.017 W m^{-1} K^{-1} (at 873 Pa) to 0.021 W m^{-1} K^{-1} (at 19,947 Pa) (Wagner and Kretzschmar, 2008).

3.4. Effective thermal conductivity chart for open-system packed bed adsorbers

Changes in ETC due to the water uptake, RH and mean temperature in the open-system packed bed adsorbers are shown in Fig. 5, for SC-arranged and randomly packed beds of 0.5 and 2 mm FAM-Z02 particles. Considering the equilibrium uptake of FAM-Z02, the isorelative humidity lines and isotherms and their corresponding water uptake and effective thermal conductivity are shown in Fig. 5. ETCs are reported for temperatures of 10 to 90 °C, RH of 5 to 40%, and water uptake of 0.06 to 0.33 kg kg_{ads}^{-1}. ETCs in the open systems are higher compared to the ETCs of the closed systems, due to the higher pressure of the filling gas, which leads to lower micro-gap and macro-gap resistances (see Eqs. A 4 and A 5 in Appendix A), and higher thermal conductivity of air compared to that of the water vapour; At adsorbent temperature of 30 °C and water uptake of 0.32 kg kg_{ads}^{-1} (i.e. water vapor saturation temperature of 15 °C in closed-system, and RH of 40% in open-system), ETC of 2 mm FAM-Z02 open-system randomly packed bed is 0.149 W m^{-1} K^{-1}, while that of a closed-system is 0.065 W m^{-1} K^{-1}, and ETC of 0.5 mm FAM-Z02 randomly packed bed in an open-system is 0.126 W m^{-1} K^{-1}, while that of a closed-system is 0.042 W m^{-1}•K^{-1}.

3.5. Effect of contact pressure on the effective thermal conductivity

ETC and $TCR \cdot A$ versus the contact pressure are shown in Fig. 6, at 30 °C and water uptake of 0.32 kg kg_{ads}^{-1} for various particle diameters. Increasing the contact pressure leads to better inter-particle contacts in the packed bed and, therefore, an increase in ETC (see Fig. 6a). In contrast to ETC, $TCR \cdot A$ decreases with an increase in the contact pressure, as shown in Fig. 6b. For d_p of 0.25 mm ($d_p/L_{bed} = 0.02$), the decrease in $TCR \cdot A$ due to the increase in contact pressure from 0.7 to 1,000 kPa is 37%, from 0.006 to 0.004 K m^2 W^{-1}, while this decrease for d_p of 2 mm ($d_p/L_{bed} = 0.17$) is 31%, from 0.026 to 0.018 K m^2 W^{-1}.

3.6. Effect of particle size on the effective and total thermal conductivity

As shown in Fig. 6b, TCR increases with an increase in d_p due to the less contact points with the metal surface of heat exchanger. For d_p of 0.5 mm ($d_p \cdot L_{bed}^{-1} = 0.04$) and under contact pressure of 100 kPa, $TCR \cdot A$ is 0.008 K m^2 W^{-1} and $TCR \cdot R_{tot}^{-1}$ is 0.023, and for d_p of 2 mm ($d_p \cdot L_{bed}^{-1} = 0.17$), $TCR \cdot A$ is 0.022 K m^2 W^{-1} and $TCR \cdot R_{tot}^{-1}$ is 0.086. However, as shown in Fig. 6a, ETC of a packed bed of 0.5 mm FAM-Z02 is 0.039 W m^{-1} K^{-1} and that of a packed bed of 2 mm FAM-Z02 is 0.055 W m^{-1} K^{-1}, at 30 °C and under gas pressure of 1706 Pa and contact pressure of 100 kPa.

Total thermal conductivities of an open-system FAM-Z02 SC-arranged packed bed versus the relative particle size, $d_p \cdot L_{bed}^{-1}$, for bed thicknesses of 0.6 ($A \cdot m_{ads}^{-1} = 4.90$ m^2 kg^{-1}) to 48 mm ($A \cdot m_{ads}^{-1} = 0.06$ m^2 kg^{-1}) are shown in Fig. 7. For a constant bed thickness, k_{tot} of the packed beds with smaller $d_p \cdot L_{bed}^{-1}$ (i.e. more number of particle layers) is close to the ETC of the packed bed, and both ETC and k_{tot} increase with particle size. For higher $d_p \cdot L_{bed}^{-1}$ (i.e. less number of particle layers), the thermal contact conductance plays a more important role in the k_{tot} and decreases with an increase in the particle size, since the number of contact points decreases with particle size. Hence, an optimum particle

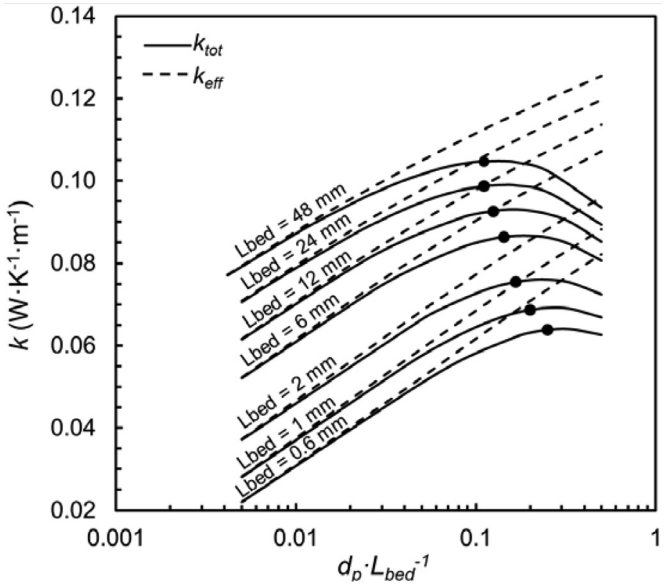

Fig. 7. Total thermal conductivity of an open-system FAM-Z02 SC-arranged packed bed at 30 °C and $\omega = 0.32$ kg kg_{ads}^{-1}.

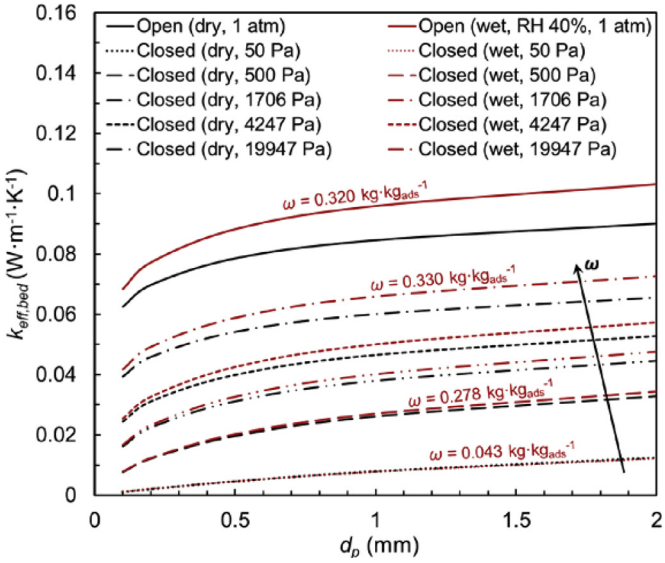

Fig. 8. ETC of dry and wet open and closed-systems SC-arranged packed bed adsorbers versus particle diameter for various gas pressures at adsorbent temperature of 30 °C.

size is observed for each bed thickness, which provides the highest k_{tot}. For instance, for 2 mm bed thickness, the optimum FAM-Z02 particle diameter which provides the highest k_{tot} is 0.34 mm. As raised by N'Tsoukpoe et al. (2014), predicting the optimum heat flow and mass flow path lengths for a certain bed volume is immensely beneficial for design and optimization of packed bed adsorbers. The presented model, which takes into account the TCR as well as the ETC for large-scale packed bed adsorbers, provides a reliable tool to predict the optimum heat flow path size (i.e. the optimum particle size) for a certain packed bed storage volume in ATES systems.

3.7. Effect of gas pressure on the thermal conductivity

As shown in Fig. 8, ETC of a dry and wet closed-system SC-arranged FAM-Z02 packed bed increases with an increase in the gas pressure. Increasing the gas pressure leads to a decrease in the mean free path of the interstitial gas (see Eq. A 23 in Appendix A) and, therefore, an increase in the ETC. Moreover, for wet packed beds, the equilibrium uptake is higher at higher gas pressures, which also leads to an increase in ETC. In a wet FAM-Z02 packed bed, by decreasing the gas pressure from 4247 (P_{sat} at 30 °C) to 1706 (P_{sat} at 15 °C) Pa, ETC decreases by 23%, from 0.043 to 0.033 W m^{-1} K^{-1}, for 0.5 mm particles, and by 16%, from 0.057 to 0.048 W m^{-1} K^{-1}, for 2 mm particles. For particle diameter of 0.5 mm, ETC of an open-system packed bed under RH of 40% is 0.079 W m^{-1} K^{-1}, while that of a closed system is 0.031 W m^{-1} K^{-1} at vapour pressure of 1706 Pa, and 0.040 W m^{-1} K^{-1} at vapour pressure of 4247 Pa.

4. Conclusions

In this study, the effective thermal conductivity of uniformly-sized packed bed adsorber was modeled as a function of water uptake, number of adsorbent layers, particle size, bed porosity, temperature, contact pressure, and interstitial gas pressure for SC and FCC arrangements, which was extended to randomly packed beds. The model was validated with the experimental results, collected by heat flow meter measurements, with a maximum relative difference of 2% for ETC and 8% for total thermal conductivity. The effective thermal conductivity of a randomly packed bed of 2 mm FAM-Z02 was between 0.188 (at 10 °C) and 0.204 W m^{-1} K^{-1} (at 80 °C). The comparison between the ETC of open-system and closed-system packed bed adsorbers showed that ETC of the open-system is higher than the ETC of the closed system. For instance, ETC of 2 mm FAM-Z02 SC-arranged open-system is 2.2 times higher than the ETC of the closed-system at 30 °C and 0.32 kg kg_{ads}^{-1} (0.1031 compared to 0.0474 W m^{-1} K^{-1}). For more realistic analysis of the heat transfer inside the packed bed adsorbers, the ETC charts were presented based on the equilibrium water uptake isotherms for both open and closed systems. Considering the dependencies of the water vapour pressure, temperature and water uptake by the equilibrium uptake isotherm, changes in ETC with water vapour pressure and water uptake were higher than its changes with the temperature in the closed systems; for 0.5 mm SC-arranged FAM-Z02 bed at 90 °C, ETC increased by 2.5 times from 0.027 to 0.068 W m^{-1} K^{-1} when water vapour pressure increases from 873 Pa (water saturation temperature of 5 °C and water uptake of 0.03 kg kg_{ads}^{-1}) to 19,947 Pa (water saturation temperature of 60 °C and water uptake of 0.26 kg kg_{ads}^{-1}). However, under 4247 Pa (water saturation temperature of 30 °C), ETC changed from 0.044 W m^{-1} K^{-1} to 0.50 W m^{-1} K^{-1} when adsorbent temperature increased from 10 °C (water uptake of 0.33 kg kg_{ads}^{-1}) to 90 °C (water uptake of 0.08 kg kg_{ads}^{-1}). Moreover, it was shown that the model could predict an optimum particle size that corresponded to the highest total thermal conductivity for a certain bed thickness, which should be considered, along with the optimum mass flow path size, for the design and optimization of packed bed adsorbers; for instance, considering 2 mm thickness for a FAM-Z02 adsorber packed bed, the optimum particle diameter which provides the highest k_{tot} is 0.34 mm.

Acknowledgements

The authors gratefully acknowledge the financial support of the Natural Sciences and Engineering Research Council of Canada (NSERC) through the Automotive Partnership Canada Grant no. APCPJ 401826–10.

Appendix A

The equations which are used in the present model to find the micro/micro-contact and micro/macro-gap resistances are listed in

Table A1
Equations used to find the thermal resistance of the unit cell, R_{cell}, (Bahrami et al., 2006; Song and Yovanovich, 1987).

Equations		Eq. number	Ref.
$R_{cell} = [\frac{1}{(1/R_{c,micro}+1/R_{g,micro})^{-1}+R_{C,macro}} + \frac{1}{R_p+R_{G,macro}}]^{-1}$	K W^{-1}	A 1	Bahrami et al. (2006)
$R_{c,micro} = [0.565\ H_{micro}(\sigma_p/m_p)]/(k_s\ F)$	K W^{-1}	A 2	Bahrami et al. (2006)
$R_{C,macro} = 1/(2\ k_s\ a_{macro})$	K W^{-1}	A 3	Bahrami et al. (2006)
$R_{g,micro} = (2\sqrt{2}\,\sigma_p\ a_2)/\{\pi\ k_g\ a_{macro}^2\ \ln(1+\frac{a_2}{a_1+M/[2\sqrt{2}\ \sigma_p\ ]})\}$	K W^{-1}	A 4	Bahrami et al. (2006)
$R_{G,macro} = \frac{2}{\pi\ k_g\ [S\ \ln(\frac{S-B}{S-A})+B-A]}$	K W^{-1}	A 5	Bahrami et al. (2006)
$k_s = \frac{2k_{p,1}\ k_{p,2}}{k_{p,1}+k_{p,2}}$	W m^{-1} K^{-1}	A 6	Bahrami et al. (2006)
$H_{micro} = c_1\ (d_v/\sigma_0)^{c_2}$	Pa	A 7	Bahrami et al. (2006)
$\sigma_0 = 1\ \mu m,\ d_v = 0.95(\sigma_p/m_p)$	M	A 8	Bahrami et al. (2006; Hegazy (1985)
$c_1 = H_{BGM}\ (4.0-5.77\kappa+4.0\kappa^2-0.61\kappa^3),\ \kappa = H_B/H_{BGM}$	Pa	A 9	Bahrami et al. (2006)
$c_2 = -0.57+0.82\kappa-0.41\kappa^2-0.06\kappa^3$		A 10	Bahrami et al. (2006)
$H_{BGM} = 3.178\ GPa,\ 1.3 \le H_B \le 7.6\ GPa$	Pa	A 11	Bahrami et al. (2006)
$m_p = \sqrt{m_{p1}^2+m_{p2}^2},\ m_{p1} = 0.076\ \sigma_{p1}^{0.52}$		A 12	Bahrami et al. (2006)
$\sigma_p = \sqrt{\sigma_{p1}^2+\sigma_{p2}^2}$	M	A 13	Bahrami et al. (2006)
$\frac{a_{macro}}{a_H} = \begin{cases} 1.605/\sqrt{P'_0} & 0.01 \le P'_0 \le 0.47 \\ 3.51-2.51P'_0 & 0.47 \le P'_0 \le 1 \end{cases}$		A 14	Bahrami et al. (2006)
$P'_0 = P_0/P_{0,H} = 1/(1+1.37\alpha(\rho_p/a_H)^{-0.075}),\ \alpha = \frac{\sigma_p\ \rho_p}{a_H^2}$		A 15	Bahrami et al. (2006)
$P_{0,H} = 1.5F/(\pi a_H^2)$	Pa	A 16	Bahrami et al. (2006)
$a_H = (0.75F\rho_p/E')^{1/3}$	M	A 17	Bahrami et al. (2006)
$E' = [(1-\nu_{p1}^2)/E_{p1}+(1-\nu_{p2}^2)/E_{p2}]^{-1}$	Pa	A 18	Bahrami et al. (2006)
$\rho_p = (1/\rho_{p1}+1/\rho_{p2})^{-1}$	M	A 19	Bahrami et al. (2006)
$a_1 = \mathrm{erfc}^{-1}(2P_0/H'),\ a_2 = \mathrm{erfc}^{-1}(0.003P_0/H') - a_1$		A 20	Bahrami et al. (2006)
$H' = c_1(1.62(\sigma_p/\sigma_0)/m_p)^{c_2}$	GPa	A 21	Bahrami et al. (2006)
$M = (\frac{2-\alpha_{T1}}{\alpha_{T1}}+\frac{2-\alpha_{T2}}{\alpha_{T2}})(\frac{2\gamma_g}{1+\gamma_g})\frac{1}{Pr}\Lambda$	M	A 22	Bahrami et al. (2006)
$\Lambda = \frac{P_{ref}}{P_g}\frac{T_g}{T_{ref}}\Lambda_{ref}$, Λ_{ref}: mean free path value at reference gas temperature T_{ref} and pressure P_{ref}	M	A 23	Bahrami et al. (2006)
$\alpha_T = \exp[-0.57(\frac{T_s-T_{ref}}{T_{ref}})](\frac{M^*}{6.8+M^*})+\frac{2.4\mu}{(1+\mu)^2}\{1-exp[-0.57(\frac{T_s-T_{ref}}{T_{ref}})]\},\ \mu = M_g/M_s$		A 24	Song and Yovanovich (1987)
$M^* = \begin{cases} M_g & \text{monoatomic gas} \\ 1.4M_g & \text{diatomic/polyatomic gas} \end{cases}$	kg mol^{-1}	A 25	Song and Yovanovich (1987)
$A = 2\sqrt{\rho_p^2-a_{macro}^2},\ B = 2\sqrt{\rho_p^2-b_{macro}^2},\ S = 2(\rho_p-\omega_0)+M,\ \omega_0 = a_{macro}^2/(2\rho_p)$	m	A 26	Bahrami et al. (2006)

Table B1
Thermal conductivity of air and water vapour.

Thermal conductivity, W m^{-1} K^{-1}			
Dry air	k_a	$0.00243+7.8421\ \times 10^{-5}\ T(^\circ C)-2.0755\ \times 10^{-5}\ T(^\circ C)^2$	VDI Heat Atlas (2010)
Water vapour	k_v	$\frac{1.713\ \times 10^{-4}\ (1+0.0129\ T(\mathrm{K}))\ \sqrt{T(\mathrm{K})}}{1-[80.95/T(\mathrm{K})]}$	VDI Heat Atlas (2010)
Humid air	k_{ha}	$k_a(1-RH\frac{P_{sat}}{P_0})+k_v\ RH\ \frac{P_{sat}}{P_0}$	Tsilingiris (2018)
FAM-Z02 powder	k_s	$0.1115+2\ \times 10^{-4}\ T(^\circ C)$	Kakiuchi et al. (2004)

Table A1 (for more details, see refs. Bahrami et al. (2006); Song and Yovanovich (1987); Bahrami et al. (2006)).

Appendix B

Thermal conductivities of the dry air, water vapour, humid air and FAM-Z02 powder are calculated from the equations presented in Table B1.

References

Alsaman, A.S., Askalany, A.A., Harby, K., Ahmed, M.S., 2017. Performance evaluation of a solar-driven adsorption desalination-cooling system. Energy 128, 196–207.

Aristov, Y.I., Glaznev, I.S., Girnik, I.S., 2012. Optimization of adsorption dynamics in adsorptive chillers: Loose grains configuration. Energy 46 (1), 484–492.

Bahrami, M., Culham, J.R., Yanovich, M.M., Schneider, G.E., 2006. Review of thermal joint resistance models for nonconforming rough surfaces. Appl. Mech. Rev. 59 (1), 1.

Bahrami, M., Yovanovich, M.M., Culham, J.R., 2006. Effective thermal conductivity of rough spherical packed beds. Int. J. Heat Mass Transf. 49 (19–20), 3691–3701.

Cabeza, L.F., 2014. Advances in Thermal Energy Storage Systems: Methods and Applications. Woodhead Publishing.

Czichos, H., Saito, T., Smith, L., 2011. Springer Handbook of Metrology and Testing, Second ed. Springer.

Dawoud, B., Sohel, M.I., Freni, A., Vasta, S., Restuccia, G., 2011. On the effective thermal conductivity of wetted zeolite under the working conditions of an adsorption chiller. Appl. Therm. Eng. 31 (14–15), 2241–2246.

Do, D.D., 1998. Adsorption Analysis: Equilibria and Kinetics, 2. Imperial College Press Imperial College Press.

El-Sharkawy, I.I., Abdelmeguid, H., Saha, B.B., 2013. Towards an optimal performance of adsorption chillers: reallocation of adsorption/desorption cycle times. Int. J. Heat Mass Transf. 63, 171–182.

Frazzica, A., Füldner, G., Sapienza, A., Freni, A., Schnabel, L., 2014. Experimental and theoretical analysis of the kinetic performance of an adsorbent coating composition for use in adsorption chillers and heat pumps. Appl. Therm. Eng. 73 (1), 1022–1031.

Freni, A., Bonaccorsi, L., Calabrese, L., Caprì, A., Frazzica, A., Sapienza, A., 2015. SAPO-34 coated adsorbent heat exchanger for adsorption chillers. Appl. Therm. Eng. 82, 1–7.

Freni, A., Dawoud, B., Bonaccorsi, L., Chmielewski, S., Frazzica, A., Calabrese, L., Restuccia, G., 2015. Characterization of zeolite-based coatings for adsorption heat pumps, Cham. Springer Briefs in Applied Sciences and Technology. Springer.

Goldsworthy, M.J., 2014. Measurements of water vapour sorption isotherms for RD silica gel, AQSOA-Z01, AQSOA-Z02, AQSOA-Z05 and CECA zeolite 3A. Microporous Mesoporous Mater 196, 59–67.

Griesinger, A., Spindler, K., Hahne, E., 1999. Measurements and theoretical modelling of the effective thermal conductivity of zeolites. Int. J. Heat Mass Transf. 42 (23), 4363–4374.

Hauer, A., Fischer, F., 2011. Open adsorption system for an energy efficient dishwasher. Chem. Ing. Tech. 83 (1–2), 61–66.

Hegazy, A.A.-H., 1985. Thermal Joint Conductance of Conforming Rough Surfaces: Effect of Surface Micro-Hardness Variation. University of Waterloo.

Incropera, F.P., Dewitt, D.P., Bergman, T.L., Lavine, A.S., 2007. Fundamentals of Heat and Mass Transfer, 6th ed. John Wiley & Sons.

Kakiuchi, H., Iwade, M., Shimooka, S., Ooshima, K., 2004. Novel zeolite adsorbents and their application for AHP and Desiccant system. In: Proceedings of the IEA-Annex 17 Meeting. Beijing.

Karayacoubian, P., Bahrami, M., Culham, J.R., 2005. Asymptotic solutions of effective thermal conductivity. In: 2005 ASME International Mechanical Engineering Congress and Exposition.

Kaviany, M., 1995. Principles of Heat Transfer in Porous Media, Second Ed. Springer, New York.
Li, G., Hwang, Y., Radermacher, R., 2014. Experimental investigation on energy and exergy performance of adsorption cold storage for space cooling application. Int. J. Refrig. 44, 23–35.
Li, X.H., Hou, X.H., Zhang, X., Yuan, Z.X., 2015. A review on development of adsorption cooling–novel beds and advanced cycles. Energy Convers. Manag. 94, 221–232.
Luikov, A.V., Shashkov, A.G., Vasiliev, L.L., Fraiman, Y.E., 1968. Thermal conductivity of porous systems. Int. J. Heat Mass Transf. 11, 117–140.
Mohammed, R.H., Mesalhy, O., Elsayed, M.L., Chow, L.C., 2017. Novel compact bed design for adsorption cooling systems: parametric numerical study. Int. J. Refrig. 80, 238–251.
N'Tsoukpoe, K.E., Restuccia, G., Schmidt, T., Py, X., 2014. The size of sorbents in low pressure sorption or thermochemical energy storage processes. Energy 77, 983–998.
Palomba, V., Vasta, S., Freni, A., 2017. Experimental testing of AQSOA FAM Z02/water adsorption system for heat and cold storage. Appl. Therm. Eng. 124, 967–974.
Pistocchini, L., Garone, S., Motta, M., 2016. Air dehumidification by cooled adsorption in silica gel grains. Part I: experimental development of a prototype. Appl. Therm. Eng. 107, 888–897.
Ramzy K, A., Ashok Babu, T.P., Kadoli, R., 2011. Semi-analytical method for heat and moisture transfer in packed bed of silica gel. Int. J. Heat Mass Transf. 54 (4), 983–993.
Rezk, A.R.M., Al-Dadah, R.K., 2012. Physical and operating conditions effects on silica gel/water adsorption chiller performance. Appl. Energy 89 (1), 142–149.
Rezk, A., Al-Dadah, R.K., Mahmoud, S., Elsayed, A., 2013. Effects of contact resistance and metal additives in finned-tube adsorbent beds on the performance of silica gel/water adsorption chiller. Appl. Therm. Eng. 53 (2), 278–284.
Riffel, D.B., Wittstadt, U., Schmidt, F.P., Núñez, T., Belo, F.A., Leite, A.P.F., Ziegler, F., 2010. Transient modeling of an adsorber using finned-tube heat exchanger. Int. J. Heat Mass Transf. 53 (7–8), 1473–1482.
Rouhani, M., Bahrami, M., 2018. Effective thermal conductivity of packed bed adsorbers : Part 2– theoretical model. Int. J. Heat Mass Transf..
Rouhani, M., Huttema, W., Bahrami, M., 2016. Heat flow meter measurement of the thermal conductivity and contact resistance of FAM AQSOA-Z02 pellets between aluminium plates. In: Proceedings of the Fourth International Symposium on Innovative Materials for Processes in Energy Systems (IMPRES2016).
Rouhani, M., Huttema, W., Bahrami, M., 2018. Effective thermal conductivity of packed bed adsorbers: Part 1–Experimental study. Int. J. Heat Mass Transf. 123, 1204–1211.
Sarwar, M.K., Majumdar, P., 1995. Thermal conductivity of wet composite porous media. Heat Recover. Syst. CHP 15 (4), 369–381.
Schreiber, H., Graf, S., Lanzerath, F., Bardow, A., 2015. Adsorption thermal energy storage for cogeneration in industrial batch processes: experiment, dynamic modeling and system analysis. Appl. Therm. Eng. 89, 485–493.
Sharafian, A., Fayazmanesh, K., McCague, C., Bahrami, M., 2014. Thermal conductivity and contact resistance of mesoporous silica gel adsorbents bound with polyvinylpyrrolidone in contact with a metallic substrate for adsorption cooling system applications. Int. J. Heat Mass Transf. 79, 64–71.
Song, S., Yovanovich, M.M., 1987. Correlation of thermal accomodation coefficient for engineering surfaces. In: Proceedings of the Twenty Fourth National Heat Transfer Conference and Exhibition, pp. 107–116.
Stroud, D., 1998. The effective medium approximations: some recent developments. Superlattices Microstruct. 23 (3), 567–573.
Tien, C.L., Vafai, K., 1978. Statistical upper and lower bounds of effective thermal conductivity of fibrous insulation. In: Proceedings of the Second AIAA/ASME Thermophysics And Heat Transfer Conference.
Tsilingiris, P.T., 2018. Review and critical comparative evaluation of moist air thermophysical properties at the temperature range between 0 and 100°C for Engineering Calculations. Renew. Sustain. Energy Rev. 83, 50–63.
Tsotsas, E., Martin, H., 1987. Thermal conductivity of packed beds: a review. Chem. Eng. Process. 22 (1), 19–37.
VDI Heat Atlas, Second ed. Springer, 2010.
Wagner, W., Kretzschmar, H.-J., 2008. International SteamTables–Properties Ofwater and Steam Based On the Industrial Formulation IAPWS-IF97, Second ed. Springer-Verlag, Berlin.
Yovanovich, 2003. Thermal spreading and contact resistances. In: Bejan, A., Kraus, D. (Eds.), Heat Transfer Handbook. John Wiley and Sons Inc., New York.
Yu, N., Wang, R.Z., Wang, L.W., 2013. Sorption thermal storage for solar energy. Prog. Energy Combust. Sci. 39 (5), 489–514.
Zhu, D., Wang, S., 2002. Experimental investigation of contact resistance in adsorber of solar adsorption refrigeration. Sol. Energy 73 (3), 177–185.